Separation Science and Technology
Publication details, including instructions for authors and subscription information:
http://www.informaworld.com/smpp/title~content=t713708471

Radiolysis and Hydrolysis of Magnetically Assisted Chemical Separation Particles

B. A. Buchholz[a]; L. Nuñez[a]; G. F. Vandegrift[a]
[a] CHEMICAL TECHNOLOGY DIVISION, ARGONNE NATIONAL LABORATORY, ARGONNE, ILLINOIS, USA

To cite this Article Buchholz, B. A. , Nuñez, L. and Vandegrift, G. F.(1996) 'Radiolysis and Hydrolysis of Magnetically Assisted Chemical Separation Particles', Separation Science and Technology, 31: 14, 1933 — 1952
To link to this Article: DOI: 10.1080/01496399608001021
URL: http://dx.doi.org/10.1080/01496399608001021

SEPARATION SCIENCE AND TECHNOLOGY, **31**(14), pp. 1933–1952, 1996

Radiolysis and Hydrolysis of Magnetically Assisted Chemical Separation Particles

B. A. BUCHHOLZ, L. NUÑEZ, and G. F. VANDEGRIFT
CHEMICAL TECHNOLOGY DIVISION
ARGONNE NATIONAL LABORATORY
9700 S. CASS AVENUE, ARGONNE, ILLINOIS 60439, USA

ABSTRACT

The magnetically assisted chemical separation process is designed to separate transuranic (TRU) elements from high-level waste or TRU waste. Magnetic microparticles (1–25 μm) were coated with octyl (phenyl)-*N*,*N*-diisobutylcarbamoylmethylphosphine oxide dissolved in tributyl phosphate and tested for removing TRU elements from acidic nitrate solutions. The particles were contacted with nitric acid solutions or simulated Hanford Plutonium Finishing Plant waste solution, irradiated with a high intensity ^{60}Co γ-ray source, and evaluated for their effectiveness in removing TRU elements from 2 M HNO_3 solutions. The resistance of the coatings and magnetic cores to radiolytic damage and hydrolytic degradation was investigated by irradiating samples of particles suspended in a variety of solutions with doses of up to 5 Mrad. Transmission electron microscopy, magnetic susceptibility measurements, and physical observations of the particles and suspension solutions were used to assess physical changes to the particles. Processes that affect the surface of the particles were found to dramatically alter the binding sites for TRU in solution. Hydrolysis played a larger role than radiolysis in the degradation of the extraction capacity of the particles.

INTRODUCTION

The objective of this study was to assess the robustness of magnetically assisted chemical separation (MACS) particles under realistic process conditions by determining the effects of radiation and acid exposure on extraction capability. The MACS process removes transuranic (TRU) elements from aqueous nitric acid solutions by extracting them into a selec-

tive organic coating adsorbed onto a magnetic particle core. Based upon the transuranic extraction (TRUEX) process, the organic coating consists of a neutral bifunctional organophosphorous extractant, octyl (phenyl)-*N*,*N*-diisobutyl-carbamoylmethylphosphine oxide (CMPO), dissolved in tributyl phosphate (TBP) (1). The particles consist of a crosslinked polyacrylamide (*N*,*N*-methylene-bis-acrylamide), entrapping charcoal, and magnetite (Fe_3O_4) in a 1:1:1 weight ratio.

The MACS process is designed to separate and concentrate TRU elements from high-level waste (HLW) or TRU waste. The process concentrates TRU elements in a small volume without producing a large secondary waste stream. The coated particles are added to the TRU waste solution in a processing tank or column, mixed thoroughly, and recovered with a magnet. The MACS system is potentially a multistage process in which the number of stages required is based upon the extraction efficiency of the system and the level of TRU activity in the feed solution. Reduction of TRU activity below 3.7×10^6 Bq·kg^{-1} (100 nCi/g) in the waste solution should allow its disposal as low-level waste (LLW), greatly reducing disposal costs. The organic coating containing the TRU elements can be stripped from the particles by using a small volume of organic solvent, or the loaded particles can be vitrified and disposed as HLW. The stripped particles can be recycled by applying a fresh coating of CMPO/TBP. A thorough discussion of the MACS process applied to the removal of TRU from nitric acid solutions is presented elsewhere (2, 3).

Since CMPO extracts both actinides and lanthanides, the particles can quickly become saturated when in contact with solutions containing high concentrations of lanthanides. The plutonium finishing plant (PFP) waste is an ideal waste matrix for the MACS process because it is practically free of lanthanides. A simulant of PFP-dissolved sludge (Table 1) was used throughout this study to determine particle damage caused by TRU activity and to monitor extraction efficiency.

When the organic coating extracts TRU from the aqueous solution, the decay of extracted TRU will cause radiolytic damage to the coating and the particle core. Prolonged exposure to nitric acid produces hydrolytic damage to the coatings and dissolves exposed magnetite in the particles. The radiolysis and hydrolysis of the organic extractant coating converts some of the CMPO and TBP into other chemical species.

Descriptions of the structure (Fig. 1) and chemistry of CMPO are in the literature (1, 4–6). Although MACS is not a solvent extraction process, the behavior of CMPO should be similar to that in the TRUEX process solvent (Table 2). The radiolytic degradation of TBP is well documented (7). When the degradation products of TBP from the γ-radiolysis of TRUEX-TCE (Table 2) were analyzed (8), only dibutyl phosphoric acid

TABLE 1
Composition of PFP Dissolved Sludge Simulant[a]

Component	Concentration (mol/L)	Component	Concentration (mol/L)
H^+	1.50E+00	Pb^{2+}	5.00E−04
Al^{3+}	4.30E−01	Cr^{3+}	4.00E−04
Ca^{2+}	6.00E−02	Ni^{2+}	4.00E−04
Mg^{2+}	6.00E−02	Cu^{2+}	3.00E−04
Na^+	4.00E−02	Be^{3+}	7.00E−05
Fe^{3+}	3.00E−02	SO_4^{2-}	1.00E−02
K^+	3.00E−03	NO_3^-	3.06E+00
Mn^{2+}	3.00E−03	F^-	9.00E−02
Zn^{2+}	6.00E−04		

[a] In water.

(HDBP) and small amounts of monobutyl phosphoric acid were produced. A plethora of degradation products of CMPO from the γ-radiolysis of TRUEX-CCl_4 and TRUEX-TCE (6, 8) have been observed. The chemical bonds most often severed are those with the N atom, the P—CH_2 bond, and the CH_2—CO bond. The hydrocarbon chains, the P=O bond, and the C=O bond are least likely to suffer radiolytic damage. Models for calculating radiolytic and hydrolytic damage to the TRUEX-NPH solvent (Table 2) are reported (9). Conversion of TBP to HDBP accounted for most of the radiolytic damage to TRUEX solvents (5, 6, 8). Radiation chemical yields for the destruction of CMPO in molecules per 100 eV absorbed, G(-CMPO), in CCl_4, TCE, TRUEX-TCE, and TRUEX-NPH were determined to be 7.4 ± 1.4 (6), 5.21 ± 0.42 (8), 3.74 ± 0.36 (8), and 0.8 ± 0.2 (9), respectively.

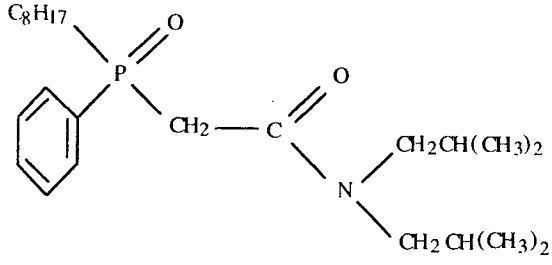

FIG. 1 Octyl(phenyl)-*N*,*N*-diisobutylcarbamoylmethylphosphine oxide (CMPO).

TABLE 2
Components of TRUEX Solvents and MACS Coating

Solvent	Diluent	CMPO concentration (mol/L)	TBP concentration (mol/L)
TRUEX-CCl_4	CCl_4	0.25	0.75
TRUEX-TCE	TCE[a]	0.25	1.0
TRUEX-NPH	NPH[b]	0.2	1.4
MACS Coating	TBP	0.58–1.5	Diluent

[a] Tetrachloroethylene.
[b] Normal paraffinic hydrocarbons, C_{12}–C_{14}.

The radiolytic and hydrolytic degradation products affect the operation of the MACS process by decreasing the concentration of CMPO and producing several acidic degradation products, which are strong extractants at low acid concentrations and thus prevent stripping of actinides under normal stripping conditions. Radiation also induces crosslinking or polymerizing chemical reactions which bond the CMPO to the charcoal and polymer and inhibit the dispersion of the particles.

Samples of MACS particles were subjected to radiolysis (10^4–10^6 rad) or hydrolysis (acid contact for 5 or 25 hours), then tested for extraction performance. Extraction performance was measured with the partitioning coefficient K_d using stock solutions of ^{241}Am in 2 M HNO_3 at 25°C. The mass balance equation of the radiotracer ^{241}Am (Eq. 1) is used to derive an expression for the K_d value. Equation (2) introduces the partitioning coefficient K_d to describe the amount of ^{241}Am on the particles in terms of its concentration in solution.

$$\mathrm{Vol_{sol}}(C_0) = \mathrm{Vol_{sol}}(C_f) + m_{part}(C_p) \quad (1)$$

$$\mathrm{Vol_{sol}}(C_0) = \mathrm{Vol_{sol}}(C_f) + (m_{part})(K_d)(C_f) \quad (2)$$

Rearranging the terms, the expression for the partitioning coefficient becomes

$$K_d = \frac{(C_0 - C_f)}{C_f} \frac{\mathrm{Vol_{sol}}}{m_{part}} \quad (3)$$

where C_0 = initial concentration of ^{241}Am in the stock solution, cpm/mL
C_f = final concentration of ^{241}Am in the contacted solution, cpm/mL
C_p = final concentration of ^{241}Am on the particles, cpm/g

Vol_{sol} = volume of solution in contact with the particles, mL (assumed not to change due to contact of particles)
m_{part} = mass of particles in contact with the solution, g
K_d = partitioning coefficient, mL/g = C_p/C_f

EXPERIMENTAL

Radiation Dose Estimates

The radiation doses delivered to the magnetic microparticles in the Argonne National Laboratory (ANL) ^{60}Co γ-ray irradiation facility were based upon estimates of the doses expected when processing waste solutions. The doses absorbed by the particles depend upon the concentration of specific isotopes adsorbed and the physical attributes such as density or average atomic number of the particles. Micrographs of the particles aided in developing assumptions about the relative concentrations of magnetite and polymer in the particles. The doses are also expressed in terms of contact cycles, where a cycle includes a complete extraction, separation, and strip process.

Since the magnetic particles are most likely to be used in removing TRU from tanks with relatively low lanthanide concentrations, the concentrations of TRU in Plutonium Finishing Plant (PFP) wastes were used to calculate activity. Most of the radioactivity in PFP waste is from the decay of ^{241}Am and several plutonium isotopes (5). Table 3 lists the radioisotopes used in calculating the doses to the magnetic particles.

Ionization is the prime mechanism of energy deposition by the emitted α-particles. An expression for the energy deposition per unit path length for heavy ions such as α-particles is given by Eq. (4) (10):

$$\left.\frac{dT}{ds}\right|_{ion} = \frac{4\pi z^2 e^4}{m_0 v^2} NZ \left(\ln \frac{2m_0 v^2}{I} - \ln(1 - \beta^2) - \beta^2\right) \frac{\text{erg}}{\text{cm}} \qquad (4)$$

TABLE 3
Concentrations of TRU Contributing to Radiation Dose in PFP Waste

Isotope[a]	Concentration (mol/L)	Specific activity (dps/L)
^{241}Am	1.6×10^{-5}	4.90×10^{8}
^{239}Pu	1.5×10^{-4}	8.25×10^{7}
^{240}Pu	9.4×10^{-6}	1.91×10^{7}
^{241}Pu	1.6×10^{-8}	1.44×10^{8}

[a] Isotope distribution of ^{239}Pu, ^{240}Pu, and ^{241}Pu is 94, 5.9, and 0.1%, respectively (5).

where T = kinetic energy of incident particle
s = path length of incident particle, cm
e = electronic charge = 4.8×10^{-10} stat C
m_0 = electronic mass = 9.11×10^{-28} g
z = charge of incident particle = 2
Z = atomic number of target
N = atomic density of target, atoms/cm^3
NZ = electron density of target, electrons/cm^3
A = atomic mass of target
v = velocity of α-particle, cm/s
c = speed of light in vacuum = 3.00×10^{10} cm/s
$\beta = v/c$
I = specific ionization = kZ = (11.5 eV)Z

The energy deposited in a target by β-particles is less concentrated than in the case of α-particles. The loss in kinetic energy per unit path length for β-particles is given by (11):

$$\frac{dE}{dx} = \frac{2\pi q^4 NZ(3 \times 10^9)^4}{E_m \beta^2 (1.6 \times 10^{-6})^2} \left[\ln\left(\frac{E_m E_k \beta^2}{I^2(1 - \beta^2)} \right) - \beta^2 \right] \frac{\text{MeV}}{\text{cm}} \qquad (5)$$

where q = charge of an electron = 1.6×10^{-19} C
N = number of absorber atoms per cm^3
Z = atomic number of absorber
NZ = electron density of absorber per cm^3
E_m = rest energy of a β-particle = 0.511 MeV
E_k = kinetic energy of the β-particle, eV
v = velocity of the β-particle, cm/s
c = speed of light in vacuum = 3.00×10^{10} cm/s
$\beta = v/c$
I = mean ionization and excitation potential of absorber = (13.5 eV)*Z

The emitted β-particles from ^{241}Pu and a neutrino share 20.8 keV. The most probable and average kinetic energy of the β-particle, approximately 1/3 E_{max} or 7.0 keV, was used when computing doses from β-particles. Ionization of target atoms is the principle mechanism for energy deposition. The dose to the magnetic particles was calculated with Eqs. (4) and (5) using the decay schemes of the isotopes in Table 3 and the following assumptions:

1. Half of the α- and β-particles are emitted into the solution, resulting in no dose to the magnetic particles.

2. Each α- and β-particle interacts with only one magnetic particle.
3. The γ-rays emitted by the TRU elements deposit an insignificant dose compared to the α- and β-particles and are thus dropped from calculations.
4. The rate of energy deposition for all isotopes is essentially the same, since the emitted α-particles are all approximately 5 MeV.
5. All TRU atoms in the initial feed solution are absorbed by the magnetic particles.
6. The process uses 10 g of magnetic particles per liter of solution.

The dose absorbed by the magnetic particles depends strongly upon the contact time per extraction, the number of extraction cycles used, the electron density of the magnetic particles, and the path length of the α- and β-particles as they traverse the absorber. Table 4 contains dose approximations for probable particle compositions, assuming 8-μm path lengths for α- and β-particles and a 1-hour contact time for each cycle in the MACS process. The average atomic number and mass of the particles is similar to pure carbon because more than 50% of the particle mass is due to carbon and the effects of hydrogen and iron cancel each other out. The doses delivered to the particles can be expressed in terms of equivalent extraction cycles. A realistic dose rate when processing PFP waste would be from 2100 to 2400 rad/h.

Materials and Methods

MACS particles used in these experiments were coated at ANL with concentrations of 0.58–1.5 M CMPO diluted in TBP. The particles were

TABLE 4
Theoretical Dose Rates for Most Probable Particle Compositions[a]

Density (g/cm³)	Atomic number	Atomic mass	Dose rate (rad/h)	10-Cycle dose (rad)	100-Cycle dose (rad)
1.8	6	12	1991	1.99E+04	1.99E+05
2.0	6	12	2188	2.19E+04	2.19E+05
2.2	6	12	2407	2.41E+04	2.41E+05
2.2	9	18	2140	2.14E+04	2.14E+05
2.5	9	18	2432	2.43E+04	2.43E+05
2.7	9	18	2627	2.63E+04	2.63E+05

[a] Assumptions include an 8-μm path length and 1-hour contact cycle time for TRU removal.

coated with 0.4–2.0 mL of solvent per gram of particles. The coating procedures can be found elsewhere (1, 2). To simulate process conditions, 30–60 mg samples of MACS particles were suspended in 2.0 mL deionized water, 0.1 M HNO_3, 2 M HNO_3, 5 M HNO_3, or PFP waste simulant. The vials used for all irradiations were blown from quartz tubing. The vials had a 10-mm outer diameter with 1-mm-thick walls and were 11–13 cm long. The hydrolysis experiments used borosilicate culture tubes with Teflon-lined screw tops.

During irradiation, the tubes were rotated end over end at 5–10 rpm to thoroughly mix the particles with the suspension solution. The solution contact times used in the hydrolysis experiments mirrored those experienced by the particles during the radiolysis experiments. The particles that received low and medium doses were in the solutions for 4–5 hours; those that received the high doses were exposed for 25 hours. The vials were rotated end over end at 8 rpm for 1 or 24 hours in the hydrolysis experiments. After irradiation or contact with hydrolysis solutions, the samples were promptly opened and the particles were separated from the suspension solutions. The particles were dried overnight on a watch glass, and samples were placed in culture tubes for measurement of the partitioning of americium, K_d(Am).

All partitioning experiments used 2 M HNO_3 at 25°C spiked with ^{241}Am. These solutions were prepared by spiking 2 M HNO_3 with concentrated ^{241}Am stock to achieve a specific activity of approximately 2×10^5 dpm/mL. The concentrations of ^{241}Am in the solutions before and after contact were measured using the 59.5 keV γ-ray emitted when ^{241}Am decays to ^{237}Np. The samples were counted with a United Technologies Packard Minaxi 5000 Series gamma counter with a 3-in. × 3-in. (7.62-cm × 7.62-cm) NaI crystal coupled to a photomultiplier tube.

All sample irradiations for this study were conducted with the 50 kCi ^{60}Co γ-ray source at ANL. Dose rates to the particles ranged from 1.1×10^5 to 2.3×10^5 rad/h to minimize acid contact time and consequently limit the effect of acid hydrolysis on the irradiated particles. The dose rates to the samples irradiated in the ^{60}Co hot cell were measured using cobalt glass. When exposed to γ-ray irradiation, the glass accumulates aggregations of imperfections that increase the optical density of the glass. The optical densities were measured with a Bausch and Lomb Spectronic 20 using light of wavelength 450 nm. Each rotor used during irradiations had two cobalt glass plates affixed to it. The average of the change in optical density of the cobalt glass was used to calculate the dose for the initial 60 or 70 minutes irradiation and to compute a dose rate. Doses were calculated to within ±10% using in-house software and approximations for the electron density of the coated particles. The particles received γ-

ray doses of 1.1×10^4 to 4.6×10^6 rad. The doses of 2.3×10^4, 2.3×10^5, and 4.6×10^6 rad correspond to 10, 100, and 2000 process cycles of treating PFP waste, respectively.

The magnetite in the MACS particles is susceptible to dissolution by the HNO_3 in solution. Particles coated with 1.5 M CMPO/TBP were placed in 2.00 mL of a variety of acid solutions ranging from 0.02 to 8 M HNO_3 for 2 weeks. Upon completion of the contact, the supernatant was removed and analyzed for iron concentration using inductively coupled plasma atomic emission spectroscopy (ICP-AES). The experiment also included a water blank that was used as the background iron concentration.

RESULTS AND DISCUSSION

Radiolysis

The radiolysis effects on the MACS particles were monitored by measuring changes in K_d(Am) with variations in radiation dose and suspension solution composition, noting changes in the physical appearances of the particles and suspension solutions, visually inspecting changes in electron micrographs of the particles, and observing the crystallization of charcoal–polymer particle cores.

The partitioning coefficient for americium decreased as the radiation dose increased (Figs. 2 and 3). The rate of decline varied with the suspen-

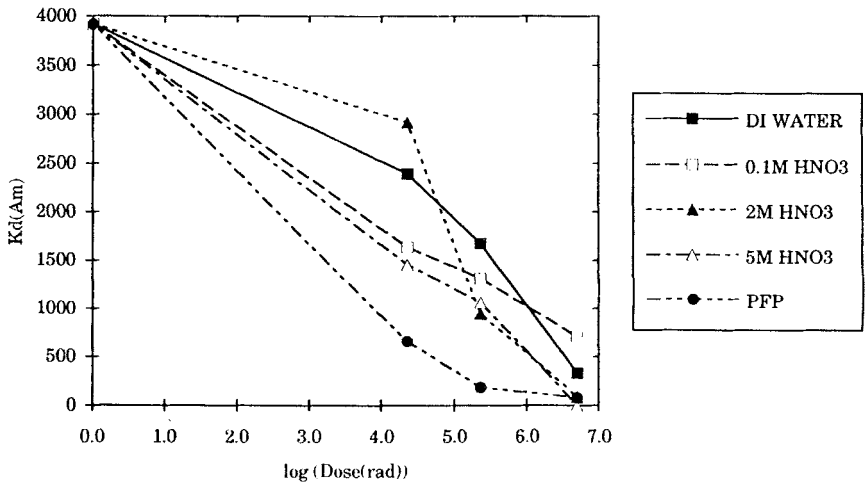

FIG. 2 K_d(Am) vs radiation dose for particles coated with 1.2 M CMPO/TBP. The series labels refer to the suspension solution during irradiation.

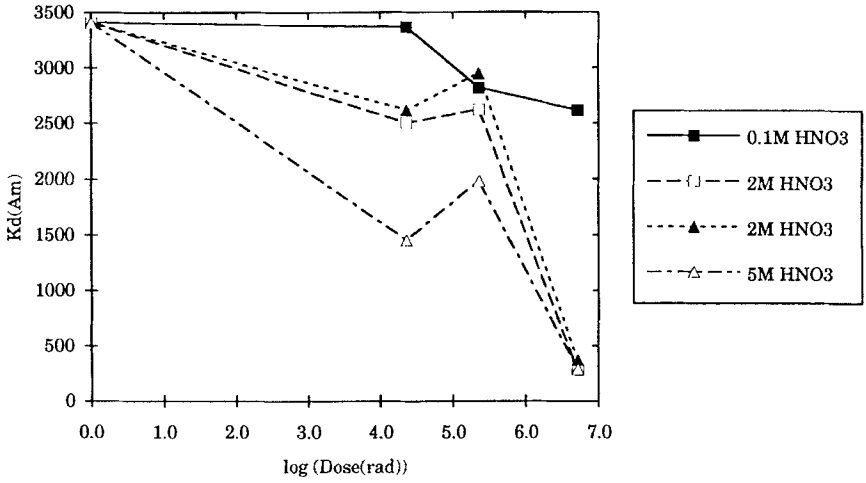

FIG. 3 K_d(Am) vs radiation dose for particles coated with 1.36 M CMPO/TBP. The series labels refer to the suspension solution during irradiation.

sion solution and the particle coating. In general, the particles that received low (1.1×10^4–2.3×10^4 rad) and medium (1.1×10^5–2.3×10^5 rad) doses retained greater extraction capability than those that received the highest dose (2.4–5 Mrad). Nonhomogeneous particle coatings complicate the comparison of distribution coefficients for different doses of the same particle coating as well as between different coatings. Based upon the scatter in K_d(Am) values measured for unirradiated particles of the same coating batches, it is reasonable to assume an uncertainty on the order of 10–20% for the K_d(Am) values of the irradiated particles.

Figures 2 and 3 depict the decrease in K_d(Am) with the increase in dose for coatings with 1.2 M CMPO/TBP and 1.36 M CMPO/TBP, respectively. The rate of decline is different for different suspension solutions, but no clear trend between the concentration of HNO_3 in the suspension solutions and the rate of decline in K_d(Am) was established.

The strongest acid contact solutions had the largest initial drop in partitioning coefficient for all the samples irradiated. Figures 2 and 3 show that the particles irradiated in 5 M HNO_3 suffered the largest initial drop in K_d(Am) for simple acid contact solutions while those suspended in 0.1 M HNO_3 appeared to retain greater extraction capability for the highest radiation doses. The PFP waste simulant is also strongly acidic (1.4 M HNO_3 and 0.1 M HF) and contains cations such as Fe^{3+} and Cr^{3+}, which

compete with Am^{3+} for binding sites on the CMPO. After the initial drop in K_d(Am) for the particles coated with 1.2 M CMPO/TBP and suspended in 5 M HNO_3, the partitioning coefficient was nearly constant for the remaining doses (Fig. 2).

The radiolysis of the suspension solutions produces radicals that can recombine in solution or attack the particles and their coatings. The nitrate anion scavenges some of the free H^+ produced during irradiation. When HNO_3 concentration was low, radiolytically produced radicals were scavenged, suppressing their attack on the particles. The stronger HNO_3 concentrations may have improved radical reduction, but damage from the high H^+ concentration probably outweighed any advantage.

The physical appearance of the suspension solutions varied with dose. The irradiated acid solutions became yellowish. The intensity of the color increased with dose and HNO_3 concentration. The stronger acids turned a deeper yellow color. The deionized water solutions did not turn yellow: They became opaque and turned white to light gray to medium gray as dose increased. The opaque solutions separated from the particles eventually cleared after several weeks, and a fine black precipitate formed on the bottom of the shell vials. The precipitate appeared to be nonmagnetized charcoal fragments.

The particles appeared to embrittle and to disperse less as dose increased. Increasing the sonication time, which is typically used to improve dispersion, did not improve dispersion of the particles. The quartz irradiation vials acquired a fine coating of particles during all irradiations. The thickness of the coating increased as dose and HNO_3 concentration increased. The quartz vials also acquired deposits of a viscous, yellow aqueous-immiscible liquid. The thickest deposits occurred in rings at the top of the suspension when the major axis of the tubes was vertical. The position of the deposits suggests that the water-immiscible phase produced during irradiation was less dense than water.

Electron micrographs of irradiated and unirradiated particles suspended in PFP waste simulant were produced. The samples were prepared for transmission electron microscopy (TEM) by ultramicrotomy to a nominal thickness of approximately 1000 nm. Semiquantitative elemental compositions were obtained by electron dispersion x-ray spectroscopy (EDS). Quantitative elemental analysis is impossible at this scale due to nonhomogeneous standard reference materials.

An uncoated sample of a MACS particle core is shown in Fig. 4(a). The charcoal–polymer material appears light gray in the TEM micrograph. The small dark regions were identified as magnetite using EDS. The magnetite was not encapsulated in the charcoal–polymer material. Electron diffraction patterns indicated that the magnetite was a crystalline material,

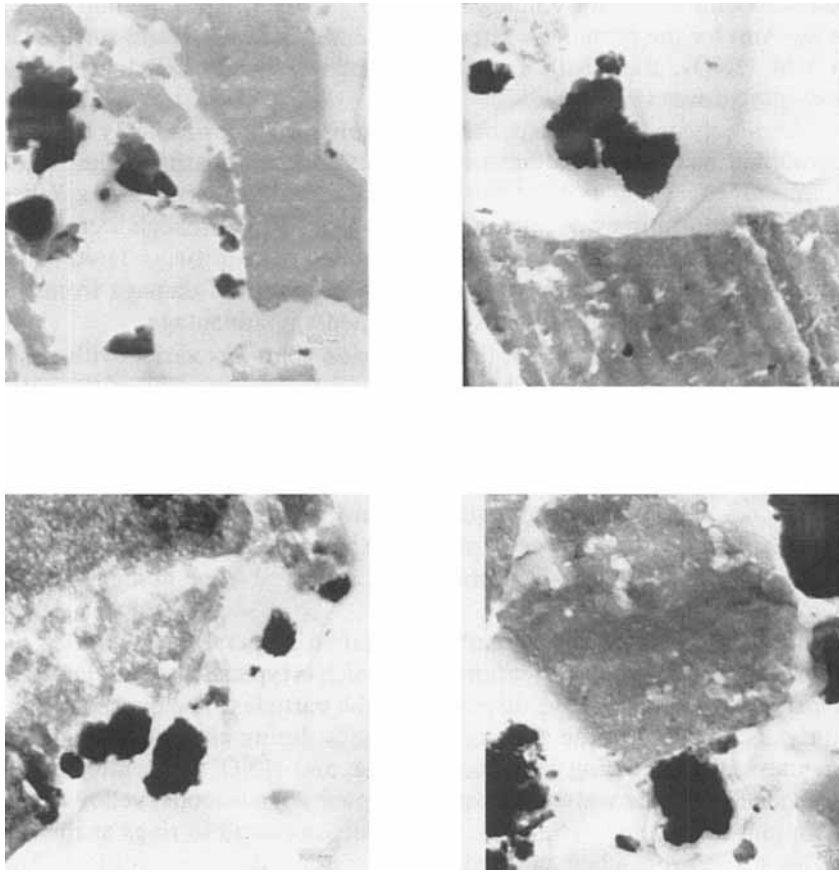

FIG. 4 TEM micrographs of charcoal–polymer–magnetite Particles. The irradiated particles were coated with 1.36 M CMPO/TBP and suspended in PFP waste simulant during γ-ray exposure. (a) Unirradiated particle. (b) Radiation dose = 1.2×10^4 rad. (c) Radiation dose = 1.2×10^5 rad. (d) Radiation dose = 2.6×10^6 rad.

but that the charcoal–polymer was amorphous. The electron diffraction patterns obtained with the electron microscope indicated crystallization of the polymer during irradiation, but could not be quantified as a function of radiation dose. Only the samples receiving doses in the 2–5 Mrad range showed evidence of short range order.

Figures 4(b), 4(c), and 4(d) are TEM micrographs of MACS particles that were irradiated with γ-ray doses of 1.2×10^4, 1.2×10^5, and $2.6 \times$

10^6 rad, respectively. The particles were coated with 1.36 M CMPO/TBP and suspended in PFP waste simulant during irradiation. These samples all exhibit some radiation damage. The damage appears as aggregations of increased contrast in the micrographs. As the dose increases, the density and size of the aggregations increase.

The EDS spectra showed concentrations of cations in the waste simulant were not distributed evenly in the coatings. The relative concentration of silicon was fairly constant in all the EDS spectra. Although the PFP simulant did not contain silicon, the HF/HNO_3 matrix is believed to have dissolved the silicon in the quartz irradiation vials. The relative concentration of phosphorous in the coatings decreased as radiation dose increased, suggesting that the phosphorous-rich coating materials (CMPO and TBP) were lost from the particles and deposited on the sides of the irradiation vials.

The magnetic properties of the particles were not adversely affected by a radiation dose in PFP waste simulant. The magnetization was measured using a superconducting quantum interfering device (SQUID) magnetometer. Magnetic saturation occurred at 0.2 T for all the particles, indicating that radiation did not effect the magnetic properties of the particles, despite evidence that some iron was dissolved by the contact solution.

Hydrolysis

The effects of radiolysis cannot be easily separated from those of hydrolysis in the system used for the irradiations. The particles were suspended in aqueous solutions at all times during irradiation. The concentration of HNO_3 in the suspension solutions did not appear to greatly affect the changes in partitioning coefficient with radiation dose. However, since the contact time of the particles and acid suspension solutions was greater for the highest doses, the decline in K_d(Am) with increasing contact time was also investigated.

Two week exposures to HNO_3 dissolved up to 22% of the iron in particles coated with 1.5 M CMPO/TBP. The concentration of iron in solution was used to determine the total fraction of iron in the particles that dissolved during contact with HNO_3 (Table 5). The concentration of iron in solution appears to reach a plateau for high acid concentrations. A shorter exposure time would probably dissolve less iron from the particles. Nevertheless, the position of the magnetite in the particles, confirmed by TEM to be on the surface rather than encapsulated, encourages dissolution in acidic environments.

The iron dissolved from the magnetite is probably in the Fe^{3+} state. Iron(III) is extracted by CMPO, so in addition to attacking the magnetic

TABLE 5
Percentage of Iron Dissolved from Particles Coated with 1.5 M CMPO/TBP during Two-Week Contact with 2.0 mL of Various HNO_3 Concentrations

HNO_3 (mol/L)	Mass (g)	Net iron dissolved (μg/mL)	Dissolved iron/particle (μg/g)	Iron dissolved (%)
0.02	0.0224	3	2.68E+02	0.1
0.98	0.0141	85	1.21E+04	5.0
2.08	0.0093	131	2.82E+04	11.7
4.97	0.0204	390	3.82E+04	15.9
8.01	0.0167	443	5.31E+04	22.0

properties of the particles, the dissolved iron competes with TRU for extraction sites. The contact time of the particles in concentrated acid solutions should be limited to prevent these adverse effects.

The hydrolysis effects on the MACS particles were measured by monitoring changes in K_d(Am) with solution contact time and noting changes in the physical appearances of the particles and solutions. The partitioning coefficient for americium from 2 M HNO_3 decreased as acid contact time increased (Figs. 5–7). The rate of decline varied with contact solution and between the different coatings. The particles in contact with the solutions for 24 hours lost much of their extraction capacity for americium. Although the nonhomogeneous particle coatings blurred the differences between the effects of different contact solutions, the partitioning coefficient suffered greater decreases in capacity for stronger acid concentrations. The change in partitioning coefficient with contact time is plotted for particles coated with 1.2, 1.36, and 0.58 M CMPO/TBP in Figs. 5, 6, and 7, respectively.

The extraction capacity of the particles coated with 1.2 M CMPO/TBP showed no dependence on the concentration of HNO_3 in solution (Fig. 5). The 50 and 90% losses in K_d(Am) for the contact times used for the irradiations suggests that hydrolysis damage was a major factor in the decline in partitioning coefficients. Figures 6 and 7 show some solution dependence in the decline in K_d(Am) with increased contact time for particles coated with 1.36 and 0.58 M CMPO, respectively. The strong acids appear to dissolve the coatings from the particles and dissolve the exposed magnetite on the surface of the charcoal/polymer cores. The loss in extraction capability is significant for all the long exposures except for the 1.36 M CMPO/TBP-coated particles contacted with 0.1 M HNO_3.

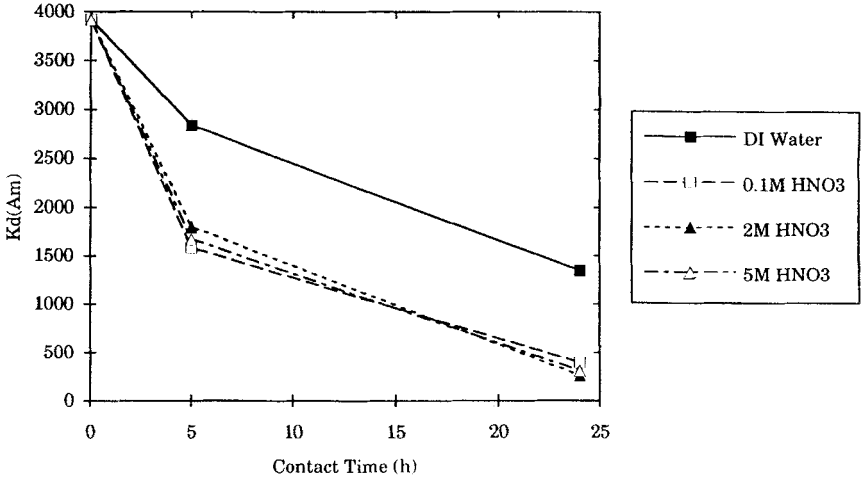

FIG. 5 Change in K_d(Am) from 2 M HNO_3 with solution contact time for particles coated with 1.2 M CMPO/TBP. The series refer to the suspension solution during contact.

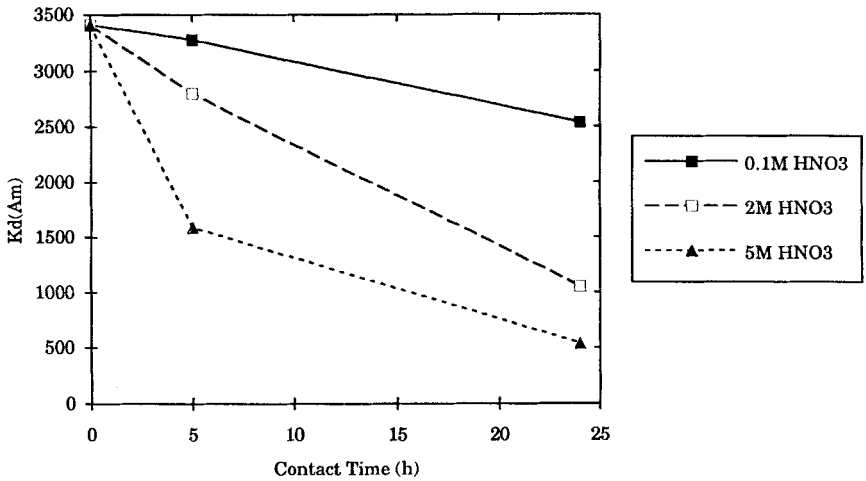

FIG. 6 Change in K_d(Am) from 2 M HNO_3 with solution contact time and aqueous phase composition for particles coated with 1.36 M CMPO/TBP. The series refer to the suspension solution during contact.

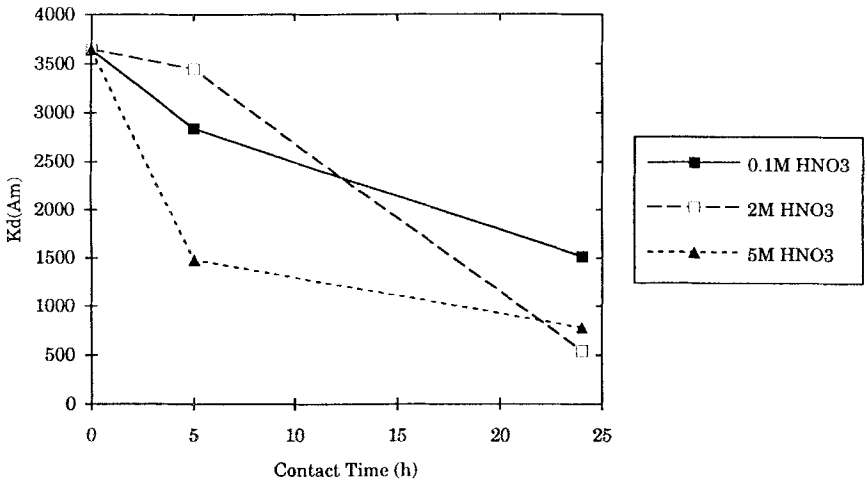

FIG. 7 Change in K_d(Am) from 2 M HNO_3 with solution contact time for particles coated with 0.58 M CMPO/TBP. The series refer to the suspension solution during contact.

The physical appearance of the suspension solutions changed with time. The strong acid solutions became pale yellow. Deposits of a viscous yellow water-immiscible liquid coated the contact vials after long exposures to the 2 and 5 M HNO_3. As in the case with the irradiation vials, the thickest deposits occurred in rings at the top of the suspension solutions when the major axis of the tubes was vertical.

The particles did not embrittle or lose dispersive ability when contacted with the acid solutions. As in the radiolysis experiments, a fine coating of particles covered the inside of the contact vials. The surface of the particles appears to be attacked by the acidic contact solutions. The yellow color in some suspension solutions and in the water-immiscible deposits to the vials is probably due to iron.

Radiolysis of the suspension solutions creates free radicals and products that can attack the coatings and surface-exposed magnetite on the particles. The radiation products produce hydrolytic effects, enhancing the behavior of the original solutions. Radiolysis of aqueous solutions produces numerous intermediate and final products (12–14). These products may strongly influence the desorption of the coatings from the particles and the dissolution of iron in the magnetite.

The changes in K_d(Am) with radiation dose and contact time were plotted together in an effort to compare directly the effects of radiolysis and hydrolysis on the MACS particles. The particles coated with 1.36 M

CMPO/TBP were exposed to three radiation doses in three different contact solutions. The K_d(Am) value corresponding to zero contact time and the 1.0×10^2 rad dose is an average of a few measurements. The individual K_d measurements were distributed from 3300 to 3500, and the average was 3410 ± 60. This particle coating was the most homogeneous of those used in irradiations.

Figures 8–10 plot both radiolysis and hydrolysis data. The particles that received low (10^4 rad) and medium (10^5 rad) radiation doses were in contact with the suspension solutions for 4–5 hours. Those that received the highest radiation doses (10^6 rad) were in the solutions for 24 hours.

Figure 8 plots radiolysis and hydrolysis data for particles coated with 1.36 M CMPO/TBP and suspended in 0.1 M HNO_3. The partitioning coefficient for 5-hour acid exposure (3280) fell between the values for the low and medium radiation doses, 3370 and 2820, respectively. The partitioning

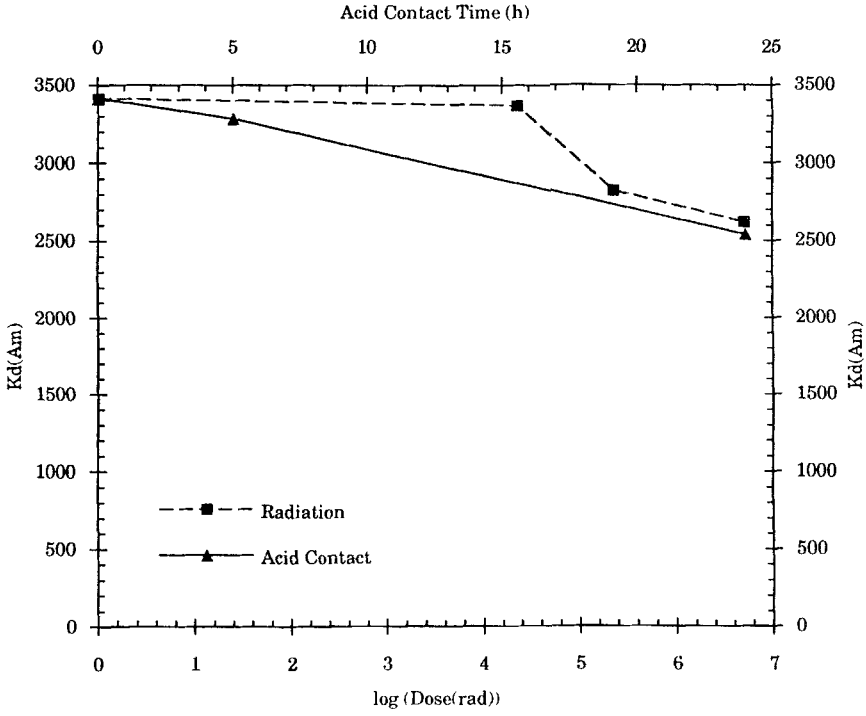

FIG. 8 Variation in K_d(Am) from 2 M HNO_3 with solution contact time and radiation dose for particles coated with 1.36 M CMPO/TBP in contact with 0.1 M HNO_3.

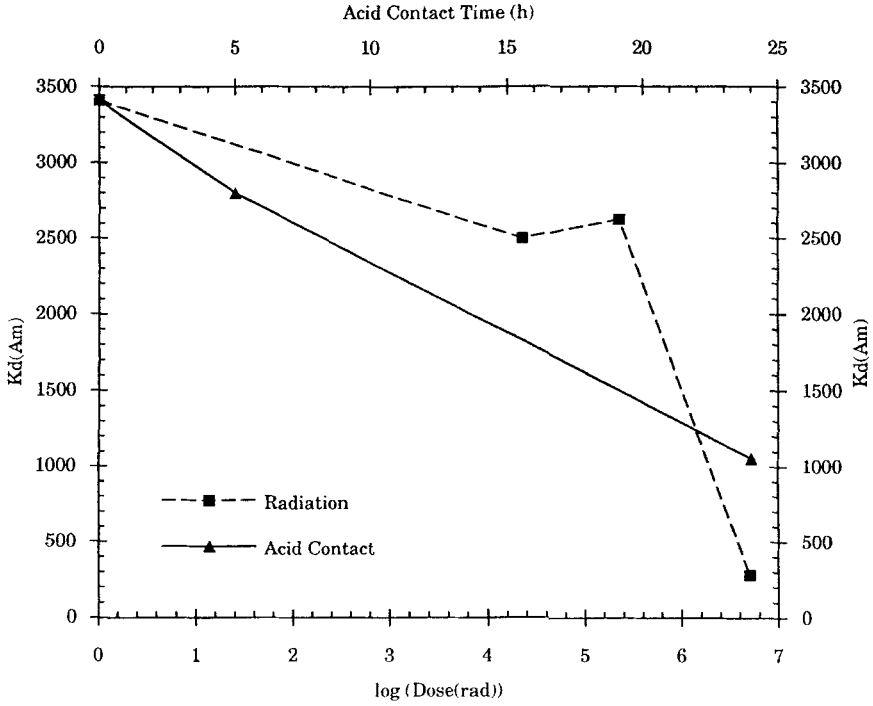

FIG. 9 Variation in K_d(Am) from 2 M HNO_3 with solution contact time and radiation dose for particles coated with 1.36 M CMPO/TBP in contact with 2 M HNO_3.

coefficient for 24-hour acid exposure (2540) fell just below the value for the high radiation dose (2620). These K_d(Am) values are essentially indistinguishable. The decline in K_d(Am) appears to be a consequence of hydrolysis rather than radiolysis. Similar comparisons can be made for the 2 and 5 M HNO_3 contact solutions (Figs. 9 and 10). The hydrolysis data mirror the radiolysis data, indicating hydrolysis is probably responsible for the observed loss in extraction capacity of the particles.

The effect of radiolysis on a typical MACS extraction cycle is minimal. The decline in K_d(Am) was insignificant for low doses. Improvements in coating procedures since the irradiation study have yielded more homogeneous coatings with consistent partitioning coefficients in the 3000–4000 mL/g range from 2 M HNO_3. The radiation dose received during a 1-hour contact cycle will have little effect on the extraction capacity of the particles.

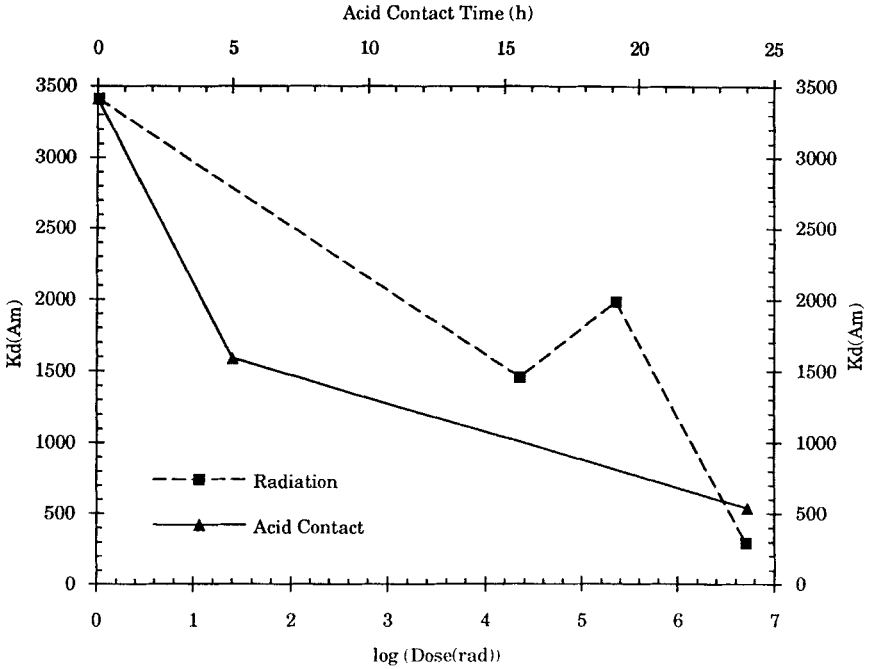

FIG. 10 Variation in K_d(Am) from 2 M HNO_3 with solution contact time and radiation dose for particles coated with 1.36 M CMPO/TBP in contact with 5 M HNO_3.

Much of the decline in K_d(Am) is associated with a loss in the CMPO/TBP coating. The loss appears to depend more strongly on the solution in contact with the particles and the length of exposure than on the radiation dose received. If the MACS process ultimately strips the organic coating loaded with TRU from the particles at the completion of a cycle and recoats them with fresh CMPO/TBP, any radiation damage will probably be negligible.

ACKNOWLEDGMENTS

This work was supported by the US Department of Energy under the Efficient Separation Processes Integrated Program (ESPIP), Contract W-31-109-Eng-38.

We appreciate the cooperation we received when coordinating activities with the Glass Shop and the Gamma Irradiation Facility in the Chemistry

Division at ANL. All the quartz vials were blown and sealed by J. Gregar in the Chemistry Division Glass Shop. Assistance provided by J. Hoh in using the ^{60}Co γ-ray source is gratefully acknowledged. The electron microscopy work was completed by C. Bradley and N. Brown in the Chemical Technology Division at ANL. Finally, we acknowledge the people who prepared the coatings on the magnetic particles used in this study, L. M. Castello, M. D. Kaminski, and M. D. Ziemer.

REFERENCES

1. G. F. Vandegrift, R. A. Leonard, M. J. Steindler, E. P. Horwitz, L. J. Basile, H. Diamond, D. G. Kalina, and L. Kaplan, *Transuranic Decontamination of Nitric Acid Solutions by the TRUEX Solvent Extraction Process—Preliminary Development Studies*, Argonne National Laboratory Report ANL-84/45, Argonne, IL, 1984.
2. L. Nuñez, B. A. Buchholz, and G. F. Vandegrift, *Sep. Sci. Technol.*, *30*, 1455 (1995).
3. L. Nuñez, B. A. Buchholz, M. Kaminski, S. B. Aase, N. R. Brown, and G. F. Vandegrift, *Ibid.*, *31*, 1393 (1996)
4. E. P. Horwitz and D. G. Kalina, *Solv. Extr. Ion Exch.*, *2*, 179 (1984).
5. R. A. Leonard, G. F. Vandegrift, D. G. Kalina, D. F. Fischer, R. W. Bane, L. Burris, E. P. Horwitz, R. Chiarizia, and H. Diamond, *The Extraction and Recovery of Plutonium and Americium from Nitric Acid Solutions by the TRUEX Process—Continuing Development Studies*, Argonne National Laboratory Report ANL-85/45, Argonne, IL, 1985.
6. R. Chiarizia and E. P. Horwitz, *Solv. Extr. Ion Exch.*, *4*, 677 (1986).
7. W. Davis Jr., *Science and Technology of Tributylphosphate*, Vol. 1 (W. W. Schulz and J. D. Navratil, Eds.), CRC Press, Boca Raton, FL, 1984, pp. 221–265.
8. K. L. Nash, R. C. Gatrone, G. A. Clark, P. G. Rickert, and E. P. Horwitz, *Sep. Sci. Technol.*, *23*, 1355 (1988).
9. N. Simonzadeh, A. M. Crabtree, L. E. Trevorrow, and G. F. Vandegrift, *Radiolysis and Hydrolysis of TRUEX-NPH Solvent*, Argonne National Laboratory Report ANL-90/14, Argonne, IL, 1992.
10. R. D. Evans, *The Atomic Nucleus*, Robert E. Krieger Publishing Company, Malabar, FL, 1955.
11. H. Cember, *Introduction to Health Physics*, 2nd ed., Pergamon Press, New York, 1983.
12. I. G. Dragonic and Z. D. Dragonic, *The Radiation Chemistry of Water*, Academic Press, New York, 1971.
13. J. W. T. Spinks and R. J. Woods, *An Introduction to Radiation Chemistry*, 3rd ed., Wiley, New York, 1990.
14. R. J. Woods and A. K. Pikaev, *Applied Radiation Chemistry: Radiation Processing*, Wiley, New York, 1994.

Received by editor September 18, 1995